



Fermi National Accelerator Laboratory

FERMILAB-Conf-90/174

Feed-Forward Compensation for Transient Beam Loading of the 805 MHz Debuncher for the Fermilab Linac Upgrade *

J. A. MacLachlan, F. E. Mills and T. Owens
Fermi National Accelerator Laboratory
P.O. Box 500
Batavia, Illinois 60510

September 7, 1990

* Presented at the 1990 Linear Accelerator Conference, Albuquerque, New Mexico, September 10-14, 1990.



Operated by Universities Research Association Inc. under contract with the United States Department of Energy

Feed-Forward Compensation for Transient Beam Loading of the 805 MHz Debuncher for the Fermilab Linac Upgrade

J. A. MacLachlan, F. E. Mills, and T. Owens

*Fermi National Accelerator Laboratory,*Box 500, Batavia IL 60510*

September 7, 1990

Abstract

The expected momentum spread from the 400 MeV upgrade of the Fermilab linac is $\pm 0.19\%$ growing to about $\pm 0.25\%$ in 63 m of beam transport to the booster synchrotron. The desired injection value is about $\pm 0.05\%$. An 805 MHz ($h=1$) debuncher is located 47 m downstream of the linac to reduce the momentum spread and the differences in mean energy between bunches. The beam pulse to the booster will vary from about 2 – 15 μs at average current of 30 – 50 mA depending on program need. During 15 μs the beam excitation of the debuncher can reach 2.2 MV/m for a three-cell cavity. This gradient is comparable to, but 90° out of phase with, the 3.85 MV/m required to minimize the momentum spread. We choose to use feed-forward compensation to control the cavity field for the entire beam pulse. We discuss some general features of transient beam loading as well as the design and detailed simulation of the compensation scheme.

Introduction

Fermilab is building an 805 MHz, 400 MeV, side-coupled H^- linac to replace the 116 to 200 MeV tanks of the present 200 MHz drift-tube linac used as an injector for the booster synchrotron.¹ Both the central energy and energy spread of the beam can vary unacceptably because of beam-induced shift of the debuncher phase. The beam parameters are summarized in Table I.

The basic scheme for the debuncher is to drift the beam so that the bunches cover somewhere between 60° – 90° of 805 MHz phase. Then the bunches pass through a cavity phased to decelerate the leading particles and accelerate trailing particles closer to the central momentum.

*Work supported by the U. S. Department of Energy under contract No. DE-AC02-76CH0300.

Beam Excitation of Debuncher

A first order calculation of the bunch lengthening along the 400 MeV transport has been made with TRACE-3D,² which accounts for the variations in longitudinal space charge force resulting from the changes in the transverse beam envelope using linearized envelope equations. The result in Fig. 1 shows both a 50 mA and a 0 mA solution which minimize momentum spread and match booster lattice functions at the injection point. The data for the debunching calculation are summarized in Table I. The solutions require $V_{eff} = E_0 T l = 1.54$ MV for 50 mA beam and 1.41 MV for $I_b = 0$.

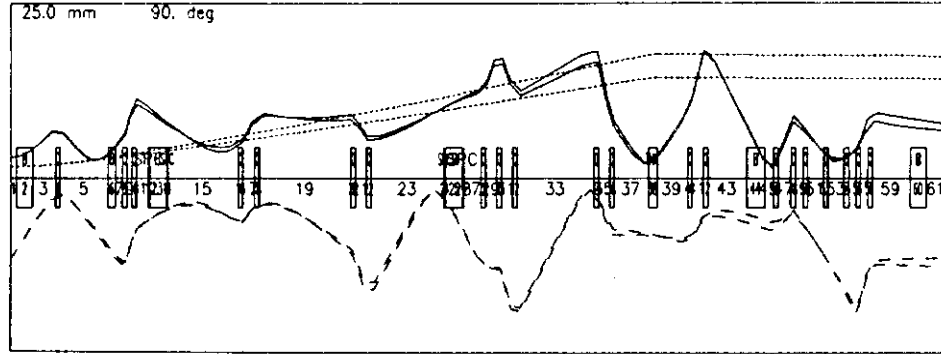


Figure 1: Beam envelope for the 400 MeV transport at $I_{beam} = 0$ and 50 mA

The 400 MeV transport design assumes a 2 cm radius minimum aperture at the debuncher. Table II gives the expected electrical properties of a 400 MeV side-coupled structure with this bore.³ The shunt impedance and Q have been reduced from the SUPERFISH result by a conventional 15%. A 50 kW TV klystron has been chosen as a suitable rf generator providing 200 kW in pulsed service. The minimum length of structure follows from the available power. For three $\beta\lambda/2$ cells the dissipation is 143 kW.

Ideal debunching requires that the cavity phase be -90° at the bunch centers. Passing bunches excite the cavity to produce a transient decelerating field shifting the phase progressively more negative. The induced voltage can be estimated by the bunch charge appearing across the gap capacity. From the stored energy given in Table II the gap capacity is 1.15 pF. Assuming the electrical energy is stored in the gap region, each bunch of 0.248 nC will generate a quadrature voltage of $\hat{V}_{beam} = q/C = 216$ V on each gap. In an extreme impulse approximation the entire beam pulse is short compared to τ_{fill} ; the beam-induced voltage would be over 2 MV.

To permit modeling the effects of the compensation scheme, detailed calculations have been carried out with time domain simulation of the beam-cavity interaction applying a code used for synchrotrons.⁴ Fig. 2 shows the quadrature voltage on the cavity as a function of time calculated by exciting an LCR cavity model with beam current pulses produced by evolution of a nominal linac bunch in the linac-to-booster drift with space charge included. The ratio of average beam radius to beampipe radius was estimated from the envelope result shown in Fig. 1. The calculated bunch length at the debuncher agreed reasonably with the

TRACE-3D result. The effect of this quadrature voltage and a fixed generator voltage on the debunching is plotted in the next two figures. Fig. 3 shows the time dependence of the mean bunch energy; the plot is offset so that the initial beam energy is in the upper lefthand corner. Fig. 4 shows how the rms energy spread increases as the phase shifts leaving the bunch outside the linear portion of the potential. The phase error after 3000 bunches at 50 mA is 19° . Fig. 5 shows superposition of an early and a late bunch. The dotted lines demark the design tolerance of 0.1% FW on $\Delta p/p$. There is some short-term fluctuation in linac beam energy; a significant benefit of the debuncher is that it reduces the range of mean energy fluctuation by the same ratio it reduces the spread within the bunch. Note, however, that the Figs. 4 and 5 results do not include spread resulting from variation in the linac energy.

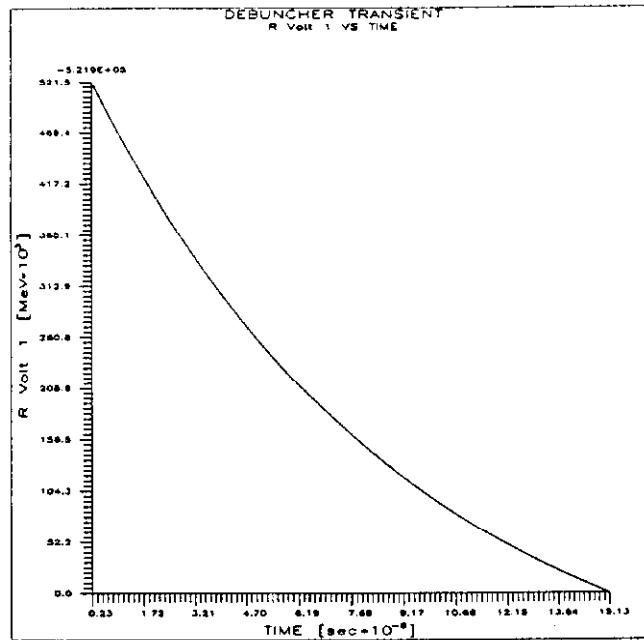


Figure 2: Quadrature voltage *vs.* time for un-corrected debuncher

Beam Loading Compensation

Beam loading degrades the debuncher performance beyond the design tolerance. A system controlling cavity phase by feedback to the rf drive can not respond fast enough. However, the timing and intensity of linac beam batches are known rather well in advance. Introducing into the rf drive an appropriate level of quadrature drive just as the beam is to arrive will cancel the effects of the beam-induced voltage during most of the pulse. The rise time on the beam current due to chopper switching is $\sim 20 - 50$ ns, whereas the klystron bandwidth is about 5 MHz. Therefore, the generator rf will be incorrect for ~ 200 ns or one

tenth of a booster turn. The error could be reduced by using a structure with lower R/Q . Greater stored energy or more rf power means that the beam-induced voltage is relatively a smaller perturbation. Unfortunately, a major improvement in Q is not possible, and high power is not economical. However, it is possible to make a major improvement by giving the correcting drive an optimum lead time on the beam pulse. The model of the feed forward scheme is shown in Fig. 6. Only the real branches of the complex envelope representation of the correction system are shown because the small phase correction to the feed-forward pulse is negligible. The output from the model is calculated with the ACSL (Advanced Computer Simulation Language); the results in Fig. 7 are normalized to $V_{\text{out}} = 1$. Fig. 7a shows an error of 0.2% in the quadrature component when the timing of the feed-forward pulse has the optimum 35 ns lead on the beam pulse. Figs. 7b and 7c show the error when the timing is off respectively by plus and minus 20 ns, the present amount of jitter on the chopper that sends the linac beam down the booster transport. Note that the scale is per mil in Fig. 7a and percent in Figs. 7b and c. One sees a maximum of 0.7% error for feed-forward of the correct amplitude within ± 20 ns of optimum timing. The time variation of the mean energy and energy spread was calculated for the case when the beam is 20 ns early; the calculation was simplified slightly by replacing the curve in Fig. 7c with a simple decaying exponential with the same peak value and time constant. On the scale of Figs. 3 and 4 the results are indistinguishable from zero.

Conclusions

Although an ideal debuncher neither delivers energy to the beam nor receives energy from it, transient beam loading shifts the debuncher phase, decelerating the beam and increasing the momentum spread. When the energy distribution must be controlled throughout the pulse, phase feedback to the klystron drive is not adequate because delays in the feedback path and bandwidth limits result in phase and amplitude errors in the debuncher field. Furthermore, beam-induced fields are comparable to those generated by the klystron; therefore, regulation factors are impractically high for the required bandwidth. However, beam timing and intensity from a linac are generally stable so that a feed-forward correction can practically eliminate phase sluing. It has been shown that the error in correction resulting from finite klystron bandwidth can be reduced substantially, a factor of three for our case, by optimally timing the correcting drive ahead of the beam pulse.

References

1. R. J. Noble, "The Fermilab Linac Upgrade", this conference
2. K. Crandall "Trace 3-D Documentation", LA-110054-MS, Los Alamos report (Aug. 87)
3. T. Jurgens, priv. comm., SUPERFISH calculation
4. S. Stahl and J. A. MacLachlan, "A User's Guide to ESME v. 7.1", Fermilab TM-1650 (26 Feb. 90), unpublished

TABLE I
Properties of the 400 MeV Linac Beam

Beam energy (kinetic)	401.46	MeV
Average beam current (\bar{I}_b)	50.	mA
Typical beam pulse	2 – 22	μ s
Bunch frequency	201.25	MHz
Frequency of rf (f)	805.0	MHz
Repetition rate	15.0	Hz
H ⁻ /bunch	1.55	$\times 10^9$
Charge/bunch (q)	0.248	nC
Bunch area (5σ)	8.17×10^{-5}	eVs
$\epsilon_{\text{trans}}(5\sigma, \text{normalized})$	6.88π	mm mrad
$\Delta p/p$ at linac (FW)	0.00373	
$\Delta\varphi$ at linac (FW)	11.8	deg
$\Delta p/p$ at booster (FW)	0.005	
Debunched $\Delta p/p$ (FW)	0.001	

TABLE II
Properties of 400 MeV SCS Cell at 805 MHz

Cell length ($\beta\lambda/2$)	0.1329	m
Cavity bore radius (r_b)	2.0	cm
Effective shunt impedance (ZT^2)	41.4	M Ω /m
Transit time factor (T)	0.831	
Quality factor (Q)	2.352×10^4	
Filling time (τ_{fill})	9.3	μ s
R/Q characteristic ratio	117.0	$\Omega(\text{true})$
Stored energy (W)	0.0101	J

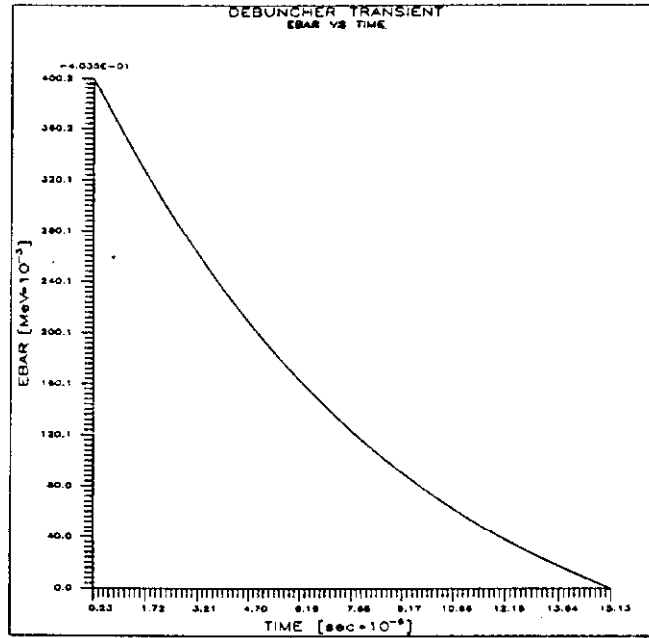


Figure 3: Mean bunch energy after debunching vs. time

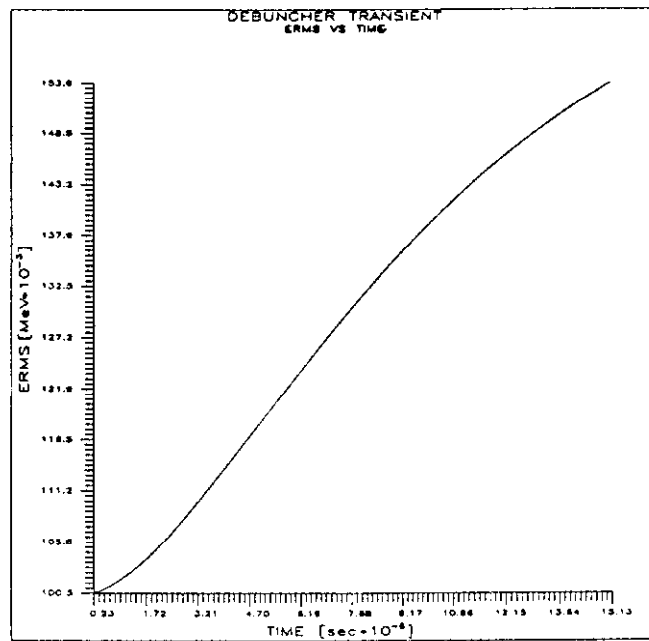


Figure 4: RMS spread of bunch energy after debunching vs. time

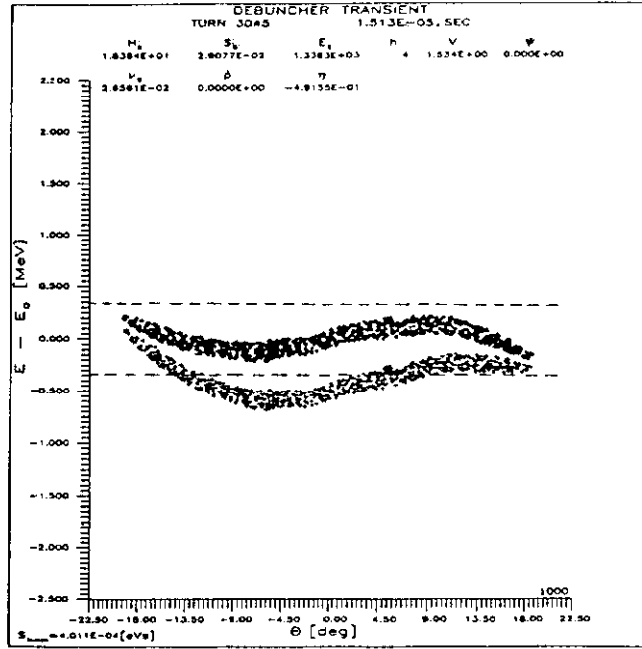


Figure 5: Bunches from 50 mA beam after debuncher — initial and 15 μ s later

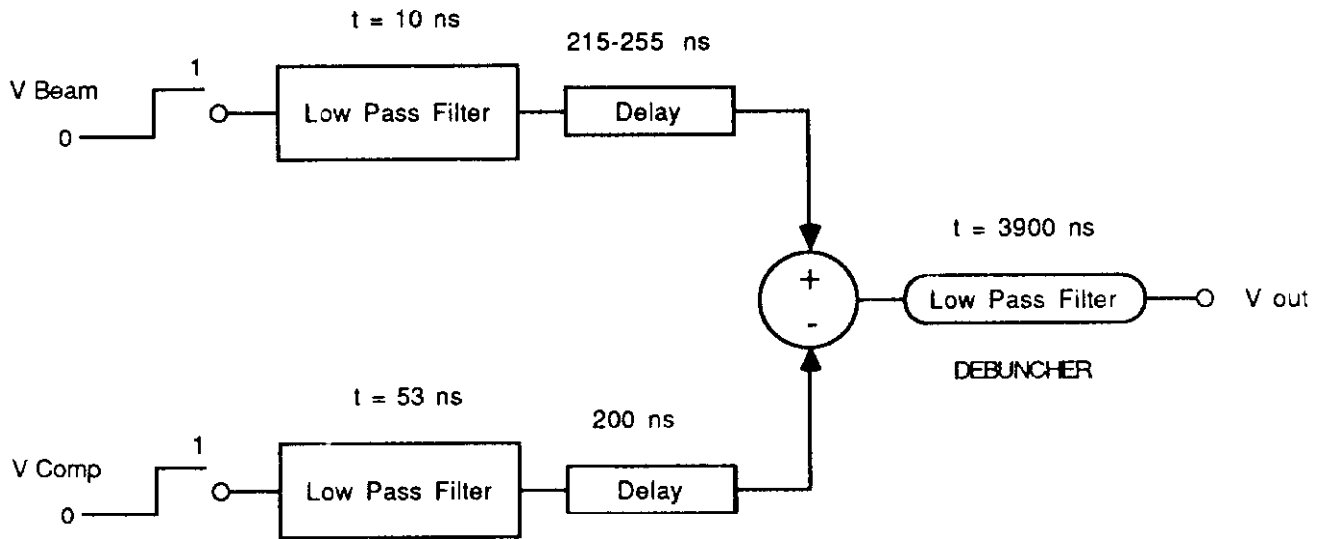


Figure 6: Model of feed-forward system — real part of complex envelope representation

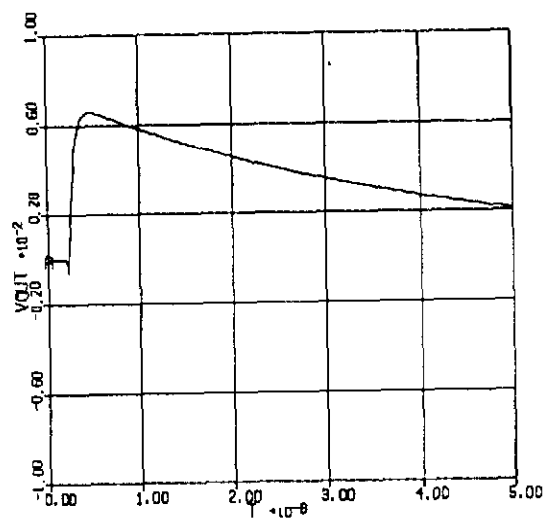
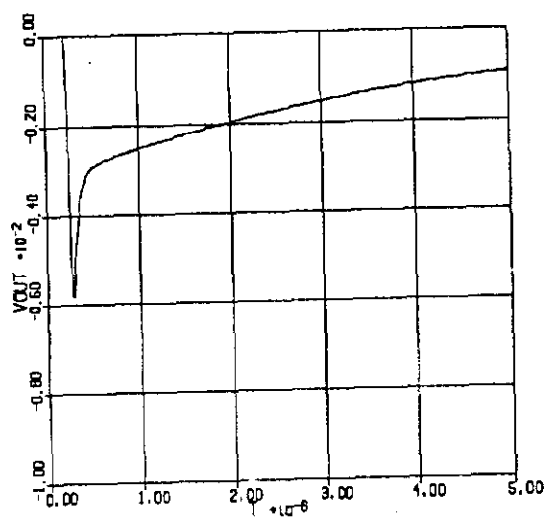
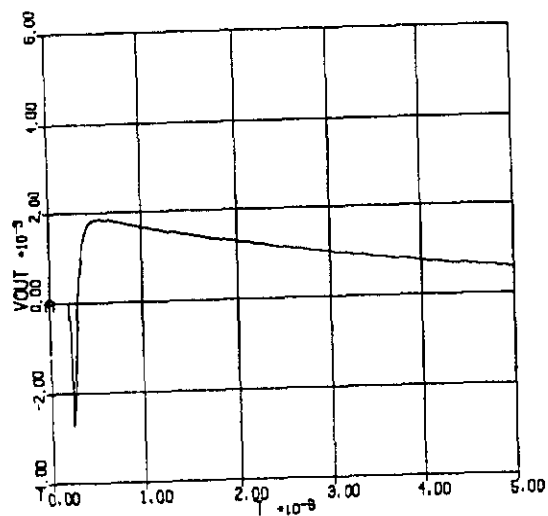


Figure 7: Fractional error in compensation vs. time for (a) 35 ns, (b) 55 ns. and (c) 15 ns beam anticipation